

<https://doi.org/10.15407/ujpe66.2.159>

A.I. POGODIN,<sup>1</sup> M.M. LUCHYNETS,<sup>1</sup> M.Y. FILEP,<sup>1</sup> A.A. KOHUTYCH,<sup>1</sup>  
T.O. MALAKHOVSKA,<sup>1</sup> O.P. KOKHAN,<sup>1</sup> M.YU. SABOV,<sup>1</sup> I.P. STUDENYAK,<sup>1</sup> P. KÚŠ<sup>2</sup>

<sup>1</sup> Uzhhorod National University

(46, Pidhirna Str., Uzhhorod, Ukraine; e-mail: studenyak@dr.com)

<sup>2</sup> Comenius University

(Mlynska dolina, Bratislava, Slovakia)

## ELECTRICAL CONDUCTIVITY AND THERMOELECTRICAL PARAMETERS OF ARGYRODITE-TYPE $\text{Cu}_{7-x}\text{PS}_{6-x}\text{I}_x$ MIXED CRYSTALS

*$\text{Cu}_{7-x}\text{PS}_{6-x}\text{I}_x$  mixed crystals were grown by the direct crystallization from a melt. The electrical conductivity is measured in the frequency range from 10 Hz to 300 kHz and in the temperature interval 293–383 K. The frequency, temperature, and compositional dependences of the electrical conductivity for  $\text{Cu}_{7-x}\text{PS}_{6-x}\text{I}_x$  mixed crystals are studied. The measurements of thermoelectric parameters of  $\text{Cu}_{7-x}\text{PS}_{6-x}\text{I}_x$  mixed crystals are carried out in the temperature interval 293–383 K. The compositional behaviors of the electrical conductivity, activation energy, Seebeck coefficient, and power factor are investigated. The interrelation between the structural, electrical, and thermoelectrical properties is analyzed.*

*Keywords:* mixed crystals, electrical conductivity, activation energy, Seebeck coefficient, power factor, compositional dependence.

### 1. Introduction

The compounds with argyrodite structure are well known firstly as the superionic conductors [1, 2]. The most investigated among the argyrodite-type compounds are  $\text{Cu}_6\text{PS}_5\text{I}$  crystals [1–3]. Due to the superionic, ferroelastic, and nonlinear-optical properties, they are advanced materials for various applications (e.g., [4]). The great possibilities for the substitution of atoms in argyrodites allow for preparing the number of solid solutions on the basis of  $\text{Cu}_6\text{PS}_5\text{I}$  crystals [3, 5, 6]. Recently, the argyrodites were obtained in the forms of composites, ceramics, and thin films [7–10]. It should be noted that, in addition to the

above-mentioned properties, representatives of the argyrodite family also exhibit thermoelectric properties. Thermoelectric materials allow the direct conversion of thermal energy into electrical one, which opens up opportunities for the recovery of excess heat into useful electricity [11,12]. However, despite their advantages, the widespread use of thermoelectric elements is limited by the low efficiency of the energy conversion process. The efficiency of energy conversion and, therefore, efficiency of thermoelectric materials can be estimated by the parameter of thermoelectric  $Q$ -factor  $ZT = S^2 \times \sigma \times T / \kappa_{\text{tot}}$  [13, 14]. The value of  $ZT$  is directly proportional to the Seebeck coefficient  $S$ , electrical conductivity  $\sigma$ , and absolute temperature  $T$  and inversely proportional to the total thermal conductivity  $\kappa_{\text{tot}}$ , which is the sum of the electron  $\kappa_{\text{el}}$  and phonon  $\kappa_{\text{lat}}$  components. Since the values of  $S$ ,  $\sigma$ , and  $\kappa_{\text{el}}$  are interconnected, the val-

© A.I. POGODIN, M.M. LUCHYNETS, M.Y. FILEP,  
A.A. KOHUTYCH, T.O. MALAKHOVSKA,  
O.P. KOKHAN, M.YU. SABOV, I.P. STUDENYAK,  
P. KÚŠ, 2021

ues of  $S$  and  $\sigma$  are linked inversely proportionally, and  $\sigma$  and  $\kappa_{\text{el}}$  are linked directly proportionally. A change of one of them often negatively affects the others. The basis of modern studies of thermoelectric materials is to improve the properties of the existing materials and search for new systems, to obtain the maximally possible efficiency of elements. An increase of  $ZT$  value can be obtained under two conditions: (i) high values of the power factor  $S^2\sigma$  (electronic component), and (ii) low values of the thermal conductivity  $\kappa_{\text{lat}}$  (phonon component). These conditions are realized in compounds corresponding to the concept of “phonon liquid–electronic crystal”, which is a continuation of the Slack theory [14]. The concept of “phonon liquid–electronic crystal” is realized by the simultaneous coexistence of a rigid covalent frame (provides high electrical conductivity) and disordered ions that behave as a liquid (provide low thermal conductivity) [15]. This enables the independent optimization of both components: electronic  $S^2\sigma$  and phonon  $\kappa_{\text{lat}}$  ones. The structural disordering of the cationic sublattice and its “liquid–like” behavior is the determining factor of the low phonon thermal conductivity  $\kappa_{\text{lat}}$  of argyrodites. The first compound of the argyrodite family, for which thermoelectric properties were presented, is  $\text{Cu}_7\text{PSe}_6$  [16]. This led to the fact that the greatest amount of information concerns the study of selenium-containing compounds with the argyrodite structure:  $\text{Cu}_8\text{GeSe}_6$  and  $\text{Ag}_8\text{GeSe}_6$  [17, 18],  $\text{Ag}_9\text{GaSe}_6$  [19],  $\text{Cu}_7\text{PSe}_6$  [20, 21]. However, the investigations of  $\text{S}^{2-} \leftrightarrow \text{Se}^{2-}$  [22] and  $\text{S}^{2-} \leftrightarrow \text{Te}^{2-}$  [23] substitutions within the anion framework of the argyrodite structure are performed nowadays. Recent studies indicate the abnormally low values of the total thermal conductivity in the interval 0.3–0.4 W/(m·K) within the temperature interval 300–600 K for  $\text{Cu}_7\text{PSe}_6$  [20, 21], 0.26 W/(m·K) at 300 K for  $\text{Ag}_9\text{GaSe}_6$  [19], 0.45 W/(m·K) at 398 K for  $\text{Ag}_8\text{SnSe}_6$  [23], 0.3 W/(m·K) at 300 K for  $\text{Cu}_8\text{GeSe}_6$  [17]. The combination of a low thermal conductivity and the predominance of the electronic component of the conductivity [21] determines the membership of the argyrodite-family compounds to the promising thermoelectric materials. Thus, the purpose of this paper is to study the electrical conductivity and thermoelectric parameters of  $\text{Cu}_{7-x}\text{PS}_{6-x}\text{I}_x$  mixed crystals, as well as to analyze the interrelation between their structural, electrical, and thermoelectrical properties.

## 2. Experimental

The synthesis of  $\text{Cu}_{7-x}\text{PS}_{6-x}\text{I}_x$  compounds was carried out in vacuum quartz ampoules from elementary components: Cu (99.999%), P (99.9999%), S (99.99995%), and pre-synthesized binary CuI taken in stoichiometric ratios using the direct one-temperature method. CuI was synthesized from elementary components Cu (99.999%) and  $\text{I}_2$  (99.9999%) taken in stoichiometric ratios in vacuumed quartz ampoules by the two-temperature method and additionally purified by the directed crystallization from the melt.  $\text{Cu}_{7-x}\text{PS}_{6-x}\text{I}_x$  mixed crystals were grown by the method of direct crystallization from a melt which is described in Ref. [24]. X-ray diffraction studies were performed, by using a DRON 4-07 diffractometer (Ni-filter,  $\text{CuK}\alpha$  radiation,  $10 < 2\theta < 80^\circ$ , scanning step is  $0.02^\circ$ , exposure is 1 s). It is shown that  $\text{Cu}_7\text{PS}_6$  and  $\text{Cu}_6\text{PS}_5\text{I}$  compounds crystallize in cubic cells,  $\text{P}2_13(\text{Cu}_7\text{PS}_6)$ ,  $\text{F-43m}(\text{Cu}_6\text{PS}_5\text{I})$ , number of formula units  $Z = 4$  [24, 25]. Therefore, in the  $\text{Cu}_7\text{PS}_6$ – $\text{Cu}_6\text{PS}_5\text{I}$  system, the formation of solid solutions is revealed. It is shown that the formation of solid solutions occurs as a result of the heterovalent substitution in the argyrodite structure with the charge compensation according to the scheme  $\text{Cu}^+ + \text{S}^{2-} \leftrightarrow \text{I}^- + \text{vak}$  [24]. Calculations of such structural parameters as the distortion index and the effective coordination number were carried out using the VESTA 3 software [26]. Investigations of the electrical conductivity of  $\text{Cu}_{7-x}\text{PS}_{6-x}\text{I}_x$  mixed crystals were carried out, by using a high-precision LCR-meter AT 2818 in the frequency range of 10 Hz–300 kHz and the temperature interval of 293–383 K on gold contacts, AC amplitude was 10 mV. The studies of the temperature dependences of the Seebeck coefficient (293–383 K) were performed with a temperature gradient not exceeding 5 K, the heating rate was 30 K/h, with independent temperature control ( $B \pm 0.15$  K) on parallel sides of the sample.

## 3. Results and Discussion

The frequency dependences of the electrical conductivity for  $\text{Cu}_7\text{PS}_6$  and  $\text{Cu}_6\text{PS}_5\text{I}$  crystals, as well as for  $\text{Cu}_{7-x}\text{PS}_{6-x}\text{I}_x$  mixed crystals, are presented in Fig. 1. The non-frequency dispersion of the electrical conductivity for all crystals under investigation in the studied frequency range is revealed. Such a frequency behavior is usually observed for the materials with

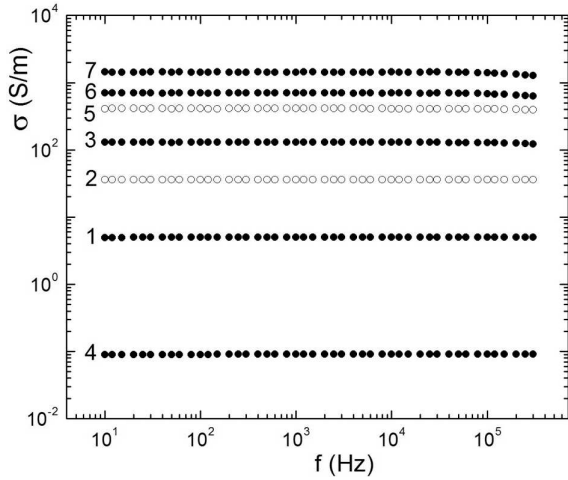


**Fig. 1.** Frequency dependences of the electrical conductivity at  $T = 303$  K for  $\text{Cu}_{7-x}\text{PS}_{6-x}\text{I}_x$  mixed crystals with  $x = 0$  (1); 0.05 (2); 0.1 (3); 0.2 (4); 0.5 (5); 0.75 (6); 1 (7)

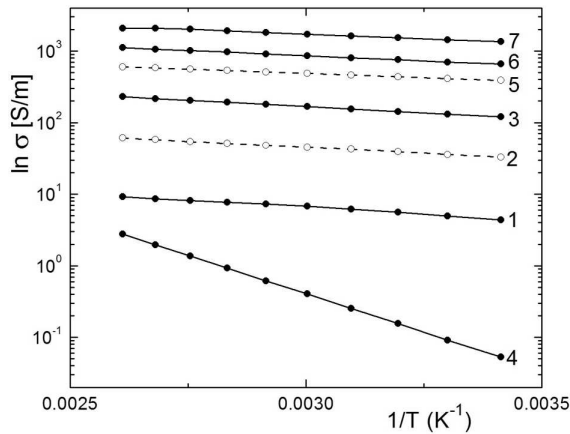


**Fig. 2.** Temperature dependences of the electrical conductivity at 1 kHz for  $\text{Cu}_{7-x}\text{PS}_{6-x}\text{I}_x$  mixed crystals with  $x = 0$  (1); 0.05 (2); 0.1 (3); 0.2 (4); 0.5 (5); 0.75 (6); 1 (7)

high electronic conductivity ( $\sigma_{\text{el}} \gg \sigma_{\text{ion}}$ ) and may be related to the ratio of electronic to ionic components of the electrical conductivity. It is shown in Ref. [27] that, for  $\text{Cu}_{7-x}\text{PS}_{6-x}\text{Br}_x$  mixed crystals, the ionic conductivity nonlinearly changes from 7.0 S/m for  $\text{Cu}_7\text{PS}_6$  to 0.5 S/m for  $\text{Cu}_6\text{PS}_5\text{Br}$  [27] in the process of heterovalent substitution. Taking the obtained values of the ionic conductivity [27] into account, the ratio of  $\sigma_{\text{el}}/\sigma_{\text{ion}}$  variates from 1.8 for  $\text{Cu}_7\text{PS}_6$  to 3810 for  $\text{Cu}_6\text{PS}_5\text{Br}$ . Thus, one can expect that the electrical conductivity dispersion can be observed at frequencies higher than  $10^8$  Hz. For the analysis of the compositional and temperature dependences, the electri-

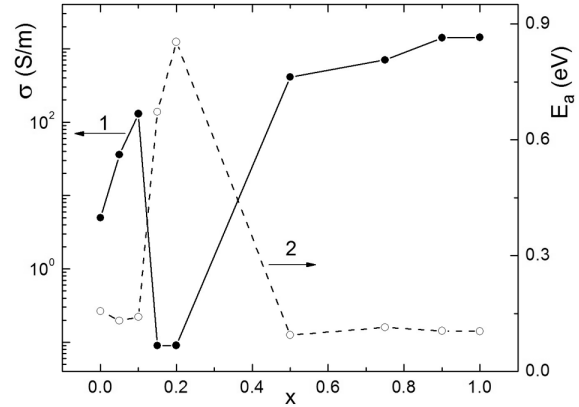


**Fig. 3.** Compositional dependences of the electrical conductivity (1) at  $T = 303$  K and the activation energy (2) for  $\text{Cu}_{7-x}\text{PS}_{6-x}\text{I}_x$  mixed crystals

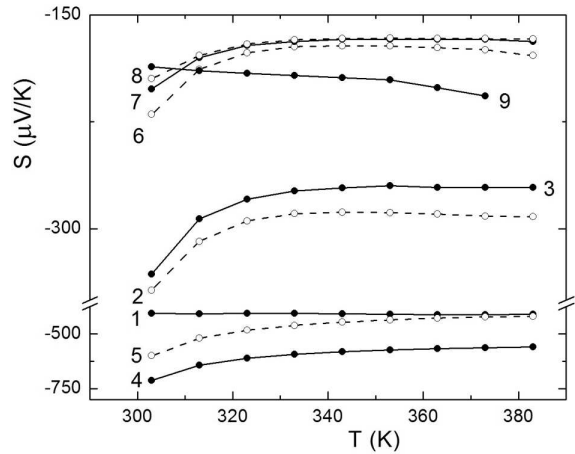


**Fig. 4.** Temperature dependences of the Seebeck coefficient for  $\text{Cu}_{7-x}\text{PS}_{6-x}\text{I}_x$  mixed crystals with  $x = 0$  (1); 0.05 (2); 0.1 (3); 0.15 (4); 0.2 (5); 0.5 (6); 0.75 (7); 0.9 (8); 1 (9)

cal conductivity values at 1 kHz are determined. The temperature dependences of the electrical conductivity are linear and described by the Arrhenius equation (Fig. 2), which allowed us to calculate the corresponding activation energies. It is shown that the compositional dependences of the electrical conductivity and activation energy for  $\text{Cu}_{7-x}\text{PS}_{6-x}\text{I}_x$  mixed crystals are nonlinear: in the process of  $\text{S}^{2-} \leftrightarrow \text{I}^-$  heterovalent substitution, a minimum of the electrical conductivity and a maximum of the activation energy are observed (Fig. 3). The temperature dependences of Seebeck coefficient for  $\text{Cu}_{7-x}\text{PS}_{6-x}\text{I}_x$  mixed crystals, obtained in the heating mode, are shown in Fig. 4. It should be noted that, for  $\text{Cu}_{7-x}\text{PS}_{6-x}\text{I}_x$  mixed crystals, the

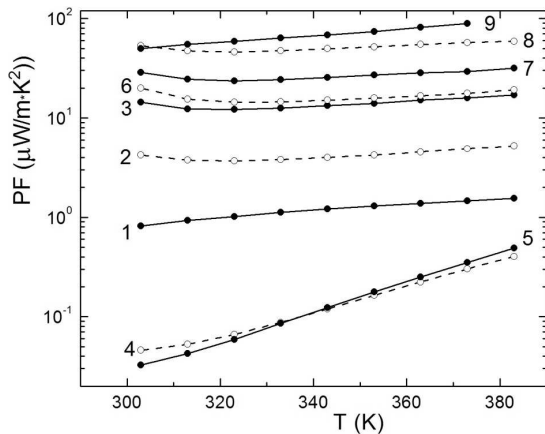


**Fig. 5.** Temperature dependences of the power factor, for  $\text{Cu}_{7-x}\text{PS}_{6-x}\text{I}_x$  mixed crystals with  $x = 0$  (1); 0.05 (2); 0.1 (3); 0.15 (4); 0.2 (5); 0.5 (6); 0.75 (7); 0.9 (8); 1 (9)

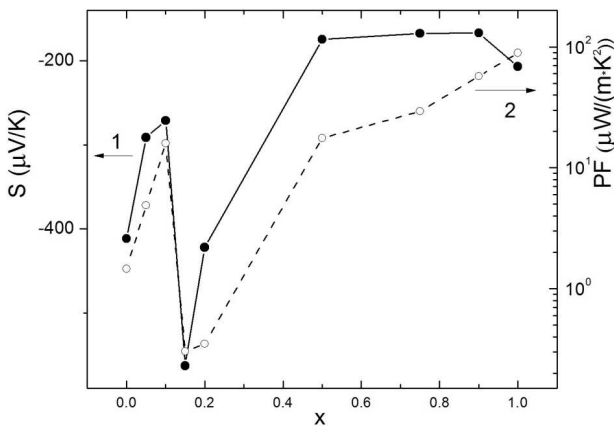


**Fig. 6.** Compositional dependences of the Seebeck coefficient (1) and PF (2) at  $T = 373$  K for  $\text{Cu}_{7-x}\text{PS}_{6-x}\text{I}_x$  mixed crystals

values of the Seebeck coefficient throughout the studied temperature interval are negative, by indicating the electronic type of the electrical conductivity ( $n$ -type). For  $\text{Cu}_7\text{PS}_6$ - $\text{Cu}_6\text{PS}_5\text{I}$  system, the maximum values of the Seebeck coefficient ( $-400 \div -700 \mu\text{V/K}$ ) are observed for  $\text{Cu}_7\text{PS}_6$  crystal, as well as for  $\text{Cu}_{6.85}\text{PS}_{5.85}\text{I}_{0.15}$  and  $\text{Cu}_{6.8}\text{PS}_{5.8}\text{I}_{0.2}$  mixed crystals, while, for  $\text{Cu}_{7-x}\text{PS}_{6-x}\text{I}_x$  mixed crystals with  $x = 0.05; 0.1; 0.5; 0.75; 0.9; 1$ , they decrease and are within  $-340 \mu\text{V/K}$  to  $-160 \mu\text{V/K}$  (Fig. 4). The power factor ( $\text{PF} = S^2 \times \sigma$ ) values for  $\text{Cu}_{7-x}\text{PS}_{6-x}\text{I}_x$  mixed crystals are calculated, and the corresponding temperature dependences are presented in Fig. 5. As a result of the analysis of the above-mentioned de-

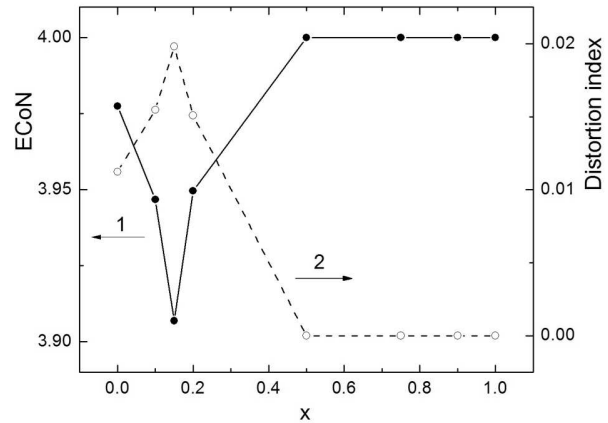


**Fig. 7.** Compositional dependences of the effective coordination number (1) and the distortion index (2) for  $\text{Cu}_{7-x}\text{PS}_{6-x}\text{I}_x$  mixed crystals

pendences, all crystals under investigation can be divided into three groups. For the first group, the value of PF does not exceed  $1 \mu\text{W}/(\text{m} \cdot \text{K}^2)$ . Despite the high values of the thermo-emf due to a low electrical conductivity,  $\text{Cu}_{6.85}\text{PS}_{5.85}\text{I}_{0.15}$  (PF from  $4.6 \times 10^{-2}$  to  $0.4 \mu\text{W}/(\text{m} \cdot \text{K}^2)$ ),  $\text{Cu}_{6.8}\text{PS}_{5.8}\text{I}_{0.2}$  (PF from  $3.3 \times 10^{-2}$  to  $0.5 \mu\text{W}/(\text{m} \cdot \text{K}^2)$ ) mixed crystals and  $\text{Cu}_7\text{PS}_6$  (PF from 0.8 to  $1.6 \mu\text{W}/(\text{m} \cdot \text{K}^2)$ ) crystals might be attributed to them. The second group comprises crystals of  $\text{Cu}_{6.95}\text{PS}_{5.95}\text{I}_{0.05}$  (PF from 4.2 to  $5.2 \mu\text{W}/(\text{m} \cdot \text{K}^2)$ ) mixed crystal for which the value of PF does not exceed  $10 \mu\text{W}/(\text{m} \cdot \text{K}^2)$ . Finally, the third group, for which the PF exceeds  $10 \mu\text{W}/(\text{m} \cdot \text{K}^2)$ , includes  $\text{Cu}_{7-x}\text{PS}_{6-x}\text{I}_x$  mixed crystals with  $x = 0.1; 0.5; 0.75; 0.9; 1$  (Fig. 5). The highest value of PF characterizes  $\text{Cu}_6\text{PS}_5\text{I}$  (PF from 49.9 to  $89.1 \mu\text{W}/(\text{m} \cdot \text{K}^2)$ ) crystal. It should be noted that the compositional behavior of the Seebeck coefficient and PF for  $\text{Cu}_{7-x}\text{PS}_{6-x}\text{I}_x$  mixed crystals is nonlinear, which is manifested as minima of the Seebeck coefficient and PF (Fig. 6). Such an anomalous behavior of the electrical conductivity, activation energy, Seebeck coefficient, and PF for  $\text{Cu}_{7-x}\text{PS}_{6-x}\text{I}_x$  mixed crystals can be explained by the compositional disordering of the anionic sublattice. To evaluate the compositional disordering, we have chosen  $[\text{PS}_4]$  tetrahedron, which is the basis of the anionic framework of argyrodite structure compounds. In the process of  $\text{S}^{2-} \leftrightarrow \text{I}^-$  heterovalent substitution in the region of concentrations  $x = 0.1 \div 0.5$ , a deformation of tetrahedrons  $[\text{PS}_4]$  is observed, which is revealed in the displacement of the

**PF at  $T = 373$  K for some binary and ternary copper chalcogenides and for  $\text{Cu}_{7-x}\text{PS}_{6-x}\text{I}_x$  mixed crystals**

Material	PF $\mu\text{W}/(\text{m} \cdot \text{K}^2)$	References
$\text{Cu}_2\text{Se}$	450.0	[28]
$\text{Cu}_2\text{S}$	87.0	[29]
$\text{Cu}_7\text{PSe}_6$	60.0	[17]
$\text{Cu}_8\text{GeSe}_6$	40.0	[18]
$\text{Cu}_8\text{GeSe}_4\text{Te}_2$	10.6	[23]
$\text{Cu}_{6.25}\text{PS}_{5.25}\text{I}_{0.75}$	29.4	[This paper]
$\text{Cu}_{6.1}\text{PS}_{5.1}\text{I}_{0.9}$	57.3	"
$\text{Cu}_6\text{PS}_5\text{I}$	89.1	"

central P atom with respect to S atoms, and, therefore, in different S-S and P-S distances. For analysis of the crystal structure deformation during the  $\text{S}^{2-} \leftrightarrow \text{I}^-$  heterovalent substitution, such parameters as the distortion index and the effective coordination number (ECoN) were employed [26]. It should be noted that the distortion index is defined as the average value of the relative deviation of the P-S bond lengths in the tetrahedron  $[\text{PS}_4]$ , whereas ECoN is defined as the sum of the contributions of all bonds to the effective coordination number [26]. For ECoN, the contribution of each atom depends on the bond length and is in the range 0-1, and in the case of increasing the distance between the central atom and the ligand atom, this number approaches zero [26]. Figure 7 shows that the variations of the effective coordination number and the distortion index in the concentration range of  $x = 0.1 \div 0.5$  for  $\text{Cu}_{7-x}\text{PS}_{6-x}\text{I}_x$  mixed crystals are nonlinear with ECoN minimum and distortion index maximum. Above  $x = 0.5$ , the values of ECoN and the distortion index are equal to 4 and 0, respectively, which testifies to the absolute symmetry of  $[\text{PS}_4]$  tetrahedra. Thus, in the concentration range of  $x \approx 0.15 \div 0.2$  for  $\text{Cu}_{7-x}\text{PS}_{6-x}\text{I}_x$  mixed crystals,  $[\text{PS}_4]$  tetrahedra are the most disordered, which leads to a strong compositional disordering of the whole anionic framework, resulting in the anomalous compositional behavior of the electrical conductivity, activation energy, Seebeck coefficient, and PF. Table shows the comparison between PF values for the materials under investigation with classical binary copper chalcogenides, namely  $\text{Cu}_2\text{Se}$  [28] and  $\text{Cu}_2\text{S}$  [29], which belong to high-temperature ther-

molectrics. In addition, the PF values for  $\text{Cu}_7\text{PSe}_6$  [16],  $\text{Cu}_8\text{GeSe}_6$  [17], and  $\text{Cu}_8\text{GeSe}_4\text{Te}_2$  [22] copper-containing argyrodites are presented in Table. It is revealed that the PF values for  $\text{Cu}_{7-x}\text{PS}_{6-x}\text{I}_x$  mixed crystals are comparable with the values for the known copper-containing chalcogenides with the argyrodite structure and binary  $\text{Cu}_2\text{S}$  (Table).

#### 4. Conclusions

$\text{Cu}_{7-x}\text{PS}_{6-x}\text{I}_x$  compounds were synthesised from the elementary components Cu, P, S and pre-synthesized binary CuI, by using the direct one-temperature method, while  $\text{Cu}_{7-x}\text{PS}_{6-x}\text{I}_x$  mixed crystals were grown by the method of direct crystallization from a melt. The measurements of the impedance and thermoelectric parameters were carried out in the temperature interval 293–383 K. The frequency, temperature, and compositional dependences of the electrical conductivity are analyzed. In the range of frequencies from of 10 Hz to 300 kHz, the non-frequency dispersion of the electrical conductivity is observed. The temperature dependences of the electrical conductivity of  $\text{Cu}_{7-x}\text{PS}_{6-x}\text{I}_x$  mixed crystals are described by the Arrhenius law. The compositional behavior of the electrical conductivity and the activation energy for  $\text{Cu}_{7-x}\text{PS}_{6-x}\text{I}_x$  mixed crystals is nonlinear. At  $\text{S}^{2-} \leftrightarrow \text{I}^-$  heterovalent substitution, the minimum of the electrical conductivity and the maximum of the activation energy are revealed. The anomalous behaviors of the electrical conductivity, activation energy, Seebeck coefficient, and power factor in  $\text{Cu}_{7-x}\text{PS}_{6-x}\text{I}_x$  mixed crystals are explained by the compositional disordering of the anionic sublattice. The interrelation between structural, electrical, and thermoelectrical properties is established.

1. W.F. Kuhs, R. Nitsche, K. Scheunemann. The argyrodites – a new family of the tetrahedrally close-packed structures. *Mater. Res. Bull.* **14**, 241 (1979).
2. T. Nilges, A. Pfitzner. A structural differentiation of quaternary copper argyrodites: Structure-property relations of high temperature ion conductors. *Z. Kristallogr.* **220**, 281 (2005).
3. I.P. Studenyak, M. Kranjčec, M.V. Kurik. Urbach rule and disordering processes in  $\text{Cu}_6\text{P}(\text{S}_{1-x}\text{Se}_x)_5\text{Br}_{1-y}\text{I}_y$  superionic conductors. *J. Phys. Chem. Solids* **67**, 807 (2006).
4. I.P. Studenyak, M. Kranjčec, Gy.Sh. Kovacs, V.V. Panko, V.V. Mitrovicij, O.A. Mikajlo. Structural disordering stud

- ies in  $\text{Cu}_{6+\delta}\text{PS}_5\text{I}$  single crystals. *Mat. Sci. & Engin. B* **97**, 34 (2003).
5. Studenyak, M. Kranjčec, Gy.S. Kovacs, I.D. Desnica-Frankovic, V.V. Panko, V.Yu. Slivka. The excitonic processes and Urbach rule in  $\text{Cu}_6\text{P}(\text{S}_{1-x}\text{Se}_x)_5\text{I}$  crystals in the sulfur-rich region. *Mat. Res. Bull.* **36**, 123 (2001).
  6. I.P. Studenyak, M. Kranjčec, O.A. Mykailo, V.V. Bilanchuk, V.V. Panko, V.V. Tovt. Crystal growth, structural and optical parameters of  $\text{Cu}_6\text{PS}_5(\text{Br}_{1-x}\text{I}_x)$  superionic conductors. *J. Optoelectr. Adv. Mat.* **3**, 879 (2001).
  7. A.F. Orliukas, E. Kazakevicius, A. Kezionis, T. Salkus, I.P. Studenyak, R.Yu. Buchuk, I.P. Prits, V.V. Panko. Preparation, electric conductivity and dielectrical properties of  $\text{Cu}_6\text{PS}_5\text{I}$ -based superionic composites. *Solid State Ionics* **180**, 183 (2009).
  8. I.P. Studenyak, V.Yu. Izai, V.I. Studenyak, O.V. Kovalchuk, T.M. Kovalchuk, P. Kopčanský, M. Timko, N. Tomašovičová, V. Zavisova, J. Miskuf, I.V. Oleinikova. Influence of  $\text{Cu}_6\text{PS}_5\text{I}$  superionic nanoparticles on the dielectric properties of 6CB liquid crystal. *Liquid Crystals* **44**, 897 (2017).
  9. T. Šalkus, E. Kazakevičius, J. Banys, M. Kranjčec, A.A. Chomolyak, Yu.Yu. Neimet, I.P. Studenyak. Influence of grain size effect on electrical properties of  $\text{Cu}_6\text{PS}_5\text{I}$  superionic ceramics. *Solid State Ionics* **262**, 597 (2014).
  10. I.P. Studenyak, M. Kranjčec, V.Yu. Izai, A.A. Chomolyak, M. Vorohta, V. Matolin, C. Cserhati, S. Kökényesi. Structural and temperature-related disordering studies of  $\text{Cu}_6\text{PS}_5\text{I}$  amorphous thin films. *Thin Solid Films* **520**, 1729 (2012).
  11. X. Shi, L. Chen. Thermoelectric materials step up. *Nature Mater.* **15**, 691 (2016).
  12. L.E. Bell. Cooling, heating, generating power, and recovering waste heat with thermoelectric systems. *Science* **321**, 1457 (2008).
  13. J. Yang, L. Xi, W. Qiu, L. Wu, X. Shi, L. Chen, J. Yang, W. Zhang, C. Uher, D.J. Singh. On the tuning of electrical and thermal transport in thermoelectrics: An integrated theory – experiment perspective. *Computational Materials* **2**, 15015 (2016).
  14. K.B. Masood, P. Kumar, R.A. Singh, J. Singh. Odyssey of thermoelectric materials: foundation of the complex structure. *J. Phys. Commun.* **2**, 062001 (2018).
  15. M. Beekman, D. Morelli, G. Nolas. Better thermoelectrics through glass-like crystals. *Nature Mater.* **14**, 1182 (2015).
  16. K.S. Weldert, W.G. Zeier, T.W. Day, M. Panthöfer, G.J. Snyder, W. Tremel. Thermoelectric transport in  $\text{Cu}_7\text{PSe}_6$  with high copper ionic mobility. *J. Am. Chem. Soc.* **136**, 12035 (2014).
  17. B. Jiang, P. Qiu, E. Eikeland, H. Chen, Q. Song, D. Ren, T. Zhang, J. Yang, B. Brummerstedt Iversen, X. Shi, L. Chen.  $\text{Cu}_8\text{GeSe}_6$ -based thermoelectric materials with an argyrodite structure. *J. Mater. Chem. C* **5**, 943 (2017).
  18. X. Shen, C.C. Yang, Y. Liu, G. Wang, H. Tan, Y.H. Tung, G. Wang, X. Lu, J. He, X. Zhou. High-temperature structural and thermoelectric study of argyrodite  $\text{Ag}_8\text{GeSe}_6$ . *ACS Appl. Mater. Interfaces* **11**, 2168 (2019).
  19. X. Qi, J. Chen, K. Guo, S. He, J. Yang, Z. Li, J. Xing, J. Hu, H. Luo, W. Zhang, J. Luo. Thermal stability of  $\text{Ag}_9\text{GaSe}_6$  and its potential as a functionally graded thermoelectric material. *Chem. Engin. J.* **374**, 494 (2019).
  20. R. Chen, P. Qiu, B. Jiang, P. Hu, Y. Zhang, J. Yang, D. Ren, X. Shia, L. Chen. Significantly optimized thermoelectric properties in high-symmetry cubic  $\text{Cu}_7\text{PSe}_6$  compounds via entropy engineering. *J. Mater. Chem. A* **6**, 6493 (2018).
  21. F. Reissig, B. Heep, M. Panthöfer, M. Wood, S. Anand, G.J. Snyder, W. Tremel. Effect of anion substitution on the structural and transport properties of argyrodites  $\text{Cu}_7\text{PSe}_{6-x}\text{S}_x$ . *Dalton Trans.* **48**, 15822 (2019).
  22. S. Schwarzmüller, D. Souchay, D. Günther, A. Gocke, I. Dovgaliuk, S.A. Miller, G.J. Snyder, O. Oeckler. Argyrodite-type  $\text{Cu}_8\text{GeSe}_{6-x}\text{Te}_x$  ( $0 < x < 2$ ): Temperature-dependent crystal structure and thermoelectric properties. *Z. Anorg. Allg. Chem.* **644**, 1915 (2018).
  23. W. Li, S. Lin, B. Ge, J. Yang, W. Zhang, Y. Pei. Low sound velocity contributing to the high thermoelectric performance of  $\text{Ag}_8\text{SnSe}_6$ . *Adv. Sci.* **3**, 1600196 (2016).
  24. I.P. Studenyak, M.M. Luchynets, V.Yu. Izai, A.I. Pogodin, O.P. Kokhan, Yu.M. Azhniuk, D.R.T. Zahn. Structure and Raman spectra of  $(\text{Cu}_6\text{PS}_5\text{I})_{1-x}(\text{Cu}_7\text{PS}_6)_x$  mixed crystals. *Semiconductor Physics, Quantum Electronics & Optoelectronics* **20**, 396 (2017).
  25. I.P. Studenyak, V.Yu. Izai, A.I. Pogodin, O.P. Kokhan, V.I. Sidey, M.Yu. Sabov, A. Kezionis, T. Šalkus, J. Banys. Structural and electrical properties of argyrodite-type  $\text{Cu}_7\text{PS}_6$  crystal. *Lit. J. Phys.* **57**, 243 (2017).
  26. K. Momma, F. Izumi. VESTA 3 for three-dimensional visualization of crystal, volumetric and morphology data. *J. Appl. Crystallogr.* **44**, 1272 (2011).
  27. A.I. Pogodin, M.J. Filep, T.O. Malakhovska, M.Yu. Sabov, V.I. Sidey, O.P. Kokhan, I.P. Studenyak. The copper argyrodites  $\text{Cu}_{7-n}\text{PS}_{6-n}\text{Br}_n$ : Crystal growth, structures and ionic conductivity. *Solid State Ionics* **341**, 115023 (2019).
  28. L.L. Zhao, X.-L. Wang, J.Y. Wang, Z.X. Cheng, S.X. Dou, J. Wang, L.Q. Liu. Superior intrinsic thermoelectric performance with ZT of 1.8 in single-crystal and melt-quenched highly dense  $\text{Cu}_{2-x}\text{Se}$  bulks. *Sci. Reports* **5**, 7671 (2015).
  29. Y. Yao, B.-P. Zhang, J. Pei, Y.-C. Liu, J.-F. Li. Thermoelectric performance enhancement of  $\text{Cu}_2\text{S}$  by Se doping leading to a simultaneous power factor increase and thermal conductivity reduction. *J. Mater. Chem. C* **5**, 7845 (2017).

Received 15.03.20

А.І. Погодін, М.М. Лучинець, М.Й. Філеп,  
А.А. Козутич, Т.О. Малаховська, О.П. Козан,  
М.Ю. Сабов, І.П. Студеняк, П. Куш

ЕЛЕКТРИЧНА ПРОВІДНІСТЬ  
ТА ТЕРМОЕЛЕКТРИЧНІ ПАРАМЕТРИ  
ТВЕРДИХ РОЗЧИНІВ ЗІ СТРУКТУРОЮ  
АРГІРОДИТУ  $\text{Cu}_{7-x}\text{PS}_{6-x}\text{I}_x$

Методом спрямованої кристалізації з розплаву вирощено монокристали твердих розчинів  $\text{Cu}_{7-x}\text{PS}_{6-x}\text{I}_x$ . Електрична провідність вимірювалася у частотному діапазоні 10 Гц–300 кГц та в інтервалі температур 293–383 К. Досліджено концентраційну, частотну та температурну за-

лежності електричної провідності монокристалів твердих розчинів  $\text{Cu}_{7-x}\text{PS}_{6-x}\text{I}_x$ . Вимірювання термоелектричних параметрів монокристалів  $\text{Cu}_{7-x}\text{PS}_{6-x}\text{I}_x$  проводились у температурному інтервалі 293–383 К. Вивчено концентраційну поведінку електричної провідності, енергії активації, коефіцієнта Зеебека та термоелектричної потужності. Проаналізовано взаємозв'язок структурних, електричних та термоелектричних властивостей твердих розчинів  $\text{Cu}_{7-x}\text{PS}_{6-x}\text{I}_x$ .

*Ключові слова:* тверді розчини, електропровідність, енергія активації, коефіцієнт Зеебека, термоелектрична потужність, концентраційна залежність.